Robust Time-Optimal Control of Flexible Structures With Parametric Uncertainty

Shin-Whar Liu
Graduate Student.

Tarunraj Singh
Assistant Professor.

SUNY at Buffalo,
Buffalo, NY 14260

The design of robust time-optimal controllers using the sensitivity concept is presented in this paper. A parameter optimization problem is solved using the Switch Time Optimization algorithm to determine a bang-bang control profile that minimizes the maneuver time subject to the constraint that the sensitivity of the final states with respect to system parameters are zero. The proposed approach is illustrated on the benchmark floating oscillator problem and a slewing flexible beam whose equations of motion are nonlinear. Simulation results illustrate the reduction of residual vibrations of the system subject to the robust control profile, compared to the time-optimal control profile.

1 Introduction

The problem of design of time-optimal controllers for flexible spacecraft is a topic of current interest which is reflected by numerous papers which address this problem for linear and nonlinear systems (Scrivener and Thompson, 1992). Singh et al. present results of time-optimal control design for rest-to-rest (1989) and spin-up maneuvers (1990) for flexible spacecraft.

Time-optimal controller are very sensitive to errors in system parameters. Therefore, development of techniques for robust time-optimal control intended to reduce residual oscillation has received increased attention in recent years (Singer and Seering, 1990; Liu and Wie, 1992; Singh and Vadali, 1994). Byers et al. (1990), applied a smooth approximation to the bang-bang control profile to deal with the rigid body mode, in conjunction with a variable structure controller to reduce the residual oscillations. Singer and Seering (1990) introduced a preshaping technique which convolved a reference input with two impulse commands to eliminate residual vibration. Upon using a series of properly arranged impulse inputs, robustness to system parameter uncertainty can be achieved. The authors also comment that as long as the system is varying slowly, the shaping technique tend to work for nonlinear systems. Singh and Vadali (1993) proposed integrating a time-delay filter designed for the linearized model to the nonlinear rigid body dynamics, and then designing a time-optimal controller for the rigid-body model of the system. Liu and Wie (1992) presented a parameter optimization approach to minimize the final maneuver time while providing robustness with respect to structural parameter uncertainty by incorporating additional constraints for a time-optimal solution. Another technique concerning structural parameter uncertainty for time-optimal control problem was proposed by Singh and Vadali (1994). They placed multiple zeros of time-delay filters to cancel the poles of system and applied a parameter optimization technique to solve the minimum time problem for both rest-to-rest and spin-up maneuvers. It should be noted that the last two approaches can only be applied to linear systems.

In this paper, a new technique which can generate robust solutions with respect to system structural uncertainty for time-optimal control of flexible spacecraft maneuvers is proposed. The new approach considers the sensitivity of states with respect to the structural uncertain parameter, as generalized state equations. These generalized states with their boundary conditions are combined with the original state equations to form a higher-order system of equations. Now, all the traditional two-point boundary value problem solving techniques can be applied to arrive at the optimal solution. The Switching Time Optimization (STO) algorithm, which was developed by Meier and Bryson (1990), will be used in this work. We first design a robust controller for a spring-mass system with stiffness uncertainty, undergoing a rest-to-rest maneuver, and compare the solution to those available in literature. This new approach can not only be applied to solve linear problems, but can also be used to address nonlinear systems with structural uncertainty.

The time-optimal control problem for the standard time-optimal and the desensitized time-optimal control problems is described in Section 2. Section 3.1 expounds the proposed technique which can be applied to solve robust time-optimal control problems with structured uncertainty. Testing the proposed approach on a spring-mass system confirms previous research in Section 3.2. The nonlinear systems of interest in this study is a flexible spacecraft which contain a rigid hub and two flexible appendages. An on-off torquer located at the center of the hub provides the required torque input for attitude control and vibration attenuation. A set of equations of motion containing the nonlinearities due to link foreshortening as well as frame rotation coupling between body axis and inertial axis are derived in Section 4.1. Numerical analysis of nonrobust and robust time-optimal control for the flexible spacecraft undergoing rest-to-rest maneuver will be presented in Section 4.2. The final section summarizes results from this study.

2 Problem Statements

The problem of designing robust time-optimal controllers for spacecraft maneuvers is stated as follows:

Determine the control that drives the system states $\underline{x}$ from their specified initial conditions $\underline{x}_0$ to their final conditions $\underline{x}_f$ while minimizing the cost function

$$J = \int_0^{t_f} 1\,dt \tag{1}$$

subject to the control constraint,

$$-\tau_{\max} \leq u \leq \tau_{\max} \tag{2}$$

and the constraint which requires the sensitivity of the final states to uncertainties in the structural parameters, be zero at the final time.

Contributed by the Dynamic Systems and Control Division for publication in the JOURNAL OF DYNAMIC SYSTEMS, MEASUREMENT, AND CONTROL. Manuscript received by the DSCD December 31, 1996. Associate Technical Editor: J. Colgate.

3 Robust Time-Optimal Control

The technique proposed in this section is motivated by the sensitivity concept. This approach provides a systematic procedure to solve the robust time-optimal control problem with structured uncertainty. Since, the proposed algorithm maintains the structure of a standard optimal control problem, its solution can be determined using the standard tools available. In this work, we use the Switching Time Optimization (STO) algorithm (Meier and Bryson, 1990), to arrive at the optimal solution. A mass-spring system and a slewing flexible structure undergoing rest-to-rest maneuvers will be used to demonstrate the proposed technique.

3.1 Proposed Approach. The objective of the proposed controller is to minimize the sensitivity of the final states of a dynamic systems to errors in estimated parameters of the system for a prescribed maneuver. To determine the sensitivity of the final states of the system

$$\dot{\underline{x}} = \underline{f}(\underline{x}, \underline{p}) \tag{3}$$

where $\underline{x} \in \mathcal{R}^n$ are the states of the system and $\underline{p}$ is a vector of parameters, we could use the direct differentiation technique leading to

$$\frac{d\dot{\underline{x}}(p)}{dp_i} = \frac{\partial \underline{f}}{\partial p_i} + \sum_{j=1}^{n} \frac{\partial \underline{f}}{\partial \underline{x}_j} \frac{\partial \underline{x}_j}{\partial p_i} \tag{4}$$

Integrating Eq. (3), in tandem with Eq. (4), leads to the sensitivity of the states.

In this work, we propose to design controllers that will force the sensitivity of the states at the final time to zero, i.e.,

$$\underline{S}_{p_i} = \frac{d\underline{x}(p)}{dp_i} = 0. \tag{5}$$

Since we want Eq. (5) to be satisfied at the final maneuver time, we consider $d\dot{\underline{x}}(p)/dp_i$ as additional state equations for a dynamic system where the additional states are

$$\underline{x}_g = \underline{S}_{p_i} = \frac{d\underline{x}(p)}{dp_i} = \int \dot{\underline{x}}_g dt \tag{6}$$

which are arrived at by integrating Eq. (4). The new state equation is formed by combining the original states and the sensitivity states together

$$\dot{\underline{y}} = \begin{bmatrix} \dot{\underline{x}} \\ \dot{\underline{x}}_g \end{bmatrix} = \begin{bmatrix} \underline{f}(\underline{x}, \underline{p}) \\ \dfrac{\partial \underline{f}}{\partial p_i} + \displaystyle\sum_{j=1}^{n} \dfrac{\partial \underline{f}}{\partial \underline{x}_j} \dfrac{\partial \underline{x}_j}{\partial p_i} \end{bmatrix} \tag{7}$$

Since the robust time-optimal control problem described above maintains the same format as the traditional time-optimal control problem, all the existing optimal control solving techniques are applicable to solve the above problem. In the following analysis, we intends to use the STO algorithm since the state equations are nonlinear.

The STO algorithm (Meier and Bryson, 1990), constructs an optimal solution based on the first-order gradient method by integrating the state equations forward in time using initial guesses of the final maneuver time and switch times of the controls. The costates are integrated backward in time, and then the terminal constraints are evaluated. If they do not satisfy the convergence criteria, improvements in the initial guesses are estimated and added to the nominal values simultaneously.

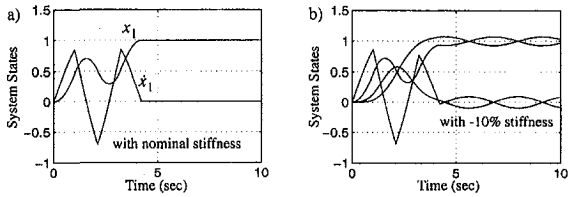

Fig. 2 Time-optimal control of two-mass-spring system

3.2 Numerical Example 1. A two-mass-spring (Fig. 1) problem, which has one rigid body and one flexible mode, will be used to demonstrate the proposed method to design robust time-optimal controllers. This problem is selected to illustrate the fact that the robust time-optimal control profile resulting from the proposed approach is identical to those presented by Liu and Wie (1992), and Singh and Vadali (1994). The equations of motion of the floating oscillator are

$$m\ddot{x}_1 + k(x_1 - x_2) = u \tag{8}$$

$$m\ddot{x}_2 + k(x_2 - x_1) = 0 \tag{9}$$

where x_1 and x_2 are the displacement of the first and second mass with respect to an inertial frame of reference. The boundary conditions for the rest-to-rest maneuver are

$$x_1(0) = x_2(0) = \dot{x}_1(0) = \dot{x}_2(0) = 0,$$

$$x_1(t_f) = x_2(t_f) = 1, \quad \text{and} \quad \dot{x}_1(t_f) = \dot{x}_2(t_f) = 0 \tag{10}$$

We intend to obtain a solution that forces the sensitivity of the states with respect to the stiffness k, to zero which leads to a robust time-optimal controller. Following the procedures discussed in Section 3.1, the parameter selected in this case is k and the sensitivity states are

$$x_{1g} = \frac{\partial x_1}{\partial k} = \int\int \ddot{x}_{1g} dt, \quad x_{2g} = \frac{\partial x_2}{\partial k} = \int\int \ddot{x}_{2g} dt,$$

$$m\ddot{x}_{1g} = -(x_1 - x_2) - k(x_{1g} - x_{2g}), \quad \text{and}$$

$$m\ddot{x}_{2g} = (x_1 - x_2) + k(x_{1g} - x_{2g}). \tag{11}$$

It is noted that $\ddot{x}_{1g} = -\ddot{x}_{2g}$; therefore we have $\dot{x}_{1g} = -\dot{x}_{2g}$ and $x_{1g} = -x_{2g}$ for this two-mass-spring system. Since two of the sensitivity states are redundant, we can simplify Eq. (11) to

$$\ddot{x}_{1g} = -(x_1 - x_2) - 2x_{1g} \tag{12}$$

where we have assumed $m = 1$ and $k = 1$ following Liu and Wie (1992).

The equations of motion used for the robust analysis are then formed by combining Eqs. (8), (9), and (12) together. The boundary conditions are modified to

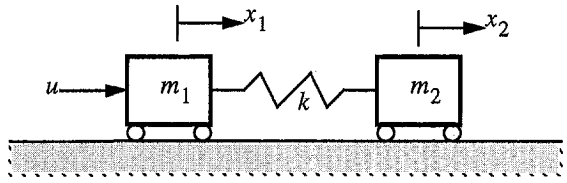

Fig. 1 Two-mass-spring system

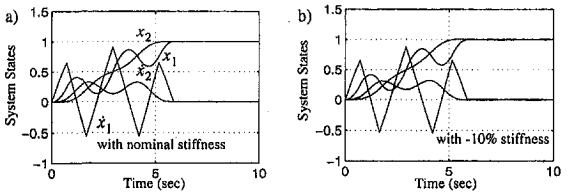

Fig. 3 Robust time-optimal control of two-mass-spring system

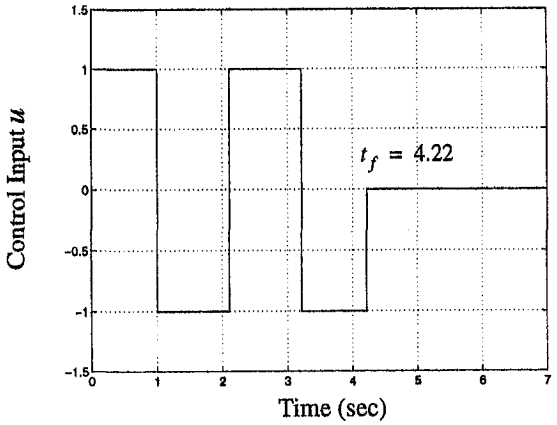

Fig. 4 Time-optimal control input

$$x_1(0) = x_2(0) = x_{1g}(0) = \dot{x}_1(0) = \dot{x}_2(0) = \dot{x}_{1g}(0) = 0,$$
$$x_1(t_f) = x_2(t_f) = 1, \quad \text{and}$$
$$\dot{x}_1(t_f) = \dot{x}_2(t_f) = \dot{x}_{1g}(t_f) = x_{1g}(t_f) = 0 \qquad (13)$$

Figure 2 and Fig. 3 present results of the application of the time-optimal control and the desensitized time-optimal controller to a system with 10 percent error in the value of the stiffness. Figures 2(*a*) illustrates the evolution of the system states using the nominal value of the stiffness. Figures 2(*b*) show that there exists a significant amount of residual vibration when the controller designed based on the nominal stiffness is applied to a system with −10 percent error in the stiffness. Figures 3(*b*) show that the application of the robust time-optimal controller to systems with −10 percent error in the stiffness reduces the residual vibration significantly. Figures 4 and 5 present the nonrobust and robust time-optimal control profiles, which are characterized by 3 and 5 switches, respectively. It is to be noted that the control profile shown in Fig. 5, which minimizes the maneuver time while minimizing the sensitivity of the final states, is identical to the controller presented by Singh and Vadali (1994). The next example will illustrate that the technique proposed in this paper can be easily applied to nonlinear systems as well.

4 Numerical Example 2

Design of controllers for large space structures undergoing large angle maneuvers which require precise pointing has been of interest to the aerospace community for the last 10–15 years. Increasing the speed of operation of these structures will excite the structural modes, and modeling the system as linear might not lead to a representative model of the system. Nonlinear terms, resulting from the deformation of the flexible beam and frame rotation coupling, cannot be neglected. The next example will address the problem of design of robust time-optimal controller for a flexible spacecraft with the aforementioned nonlinearities.

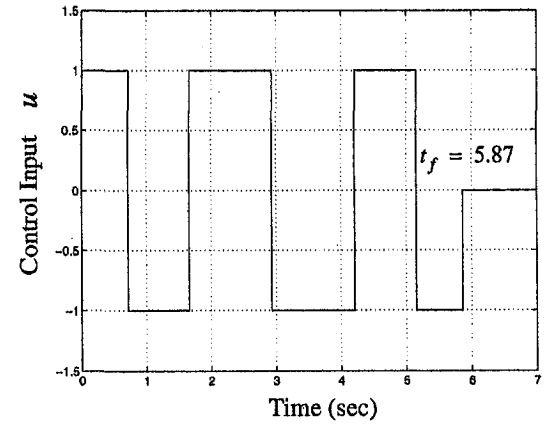

Fig. 5 Robust time-optimal control input

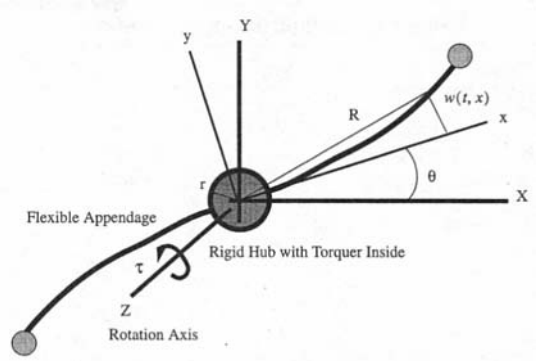

Fig. 6 Generic flexible spacecraft schematic

4.1 Equations of Motion. A schematic diagram of a generic flexible spacecraft used in this analysis is shown in Fig. 6. It consists of a rigid hub and two flexible appendages. A single momentum torquer is located in the center of hub. A body axis frame *x-y* is attached to the flexible appendage and an inertial frame *X-Y-Z* is placed in the center of hub. Vectors $\hat{i}$ and $\hat{j}$ are unit vectors in the *x-y* frame. Only small deformation of the appendages is assumed. The damping term is considered very small and is ignored.

Ignoring the foreshortening effect of the flexible appendages, the inertial position vector R, to the deformed point in the appendage can be written as

$$R = (r + x)\cdot\hat{i} + w\cdot\hat{j} \qquad (14)$$

where r is the radius of the hub, x is the location of the undeformed appendage, and w is the local deformation measured perpendicular to the x axis. The local deformation shown in Fig. 7 has the following geometric relationship

$$dx = \overline{AD} \quad \text{and} \quad \overline{AB} = \text{arc}\,(AC). \qquad (15)$$

Since we have assumed the deformation of the beam is small, we have the following approximations

$$\overline{CD} \approx ds\cdot w' \quad \text{and}$$
$$dx = \sqrt{(ds)^2 - \overline{CD}^2} = ds\sqrt{1 - (w')^2} \qquad (16)$$

where w' is the slope at point A. The binomial expansion of $\sqrt{1 - (w')^2}$, dx shown in Eq. (16) results in

$$dx = ds\cdot(1 - \tfrac{1}{2}(w')^2), \qquad (17)$$

by truncating higher-order terms.

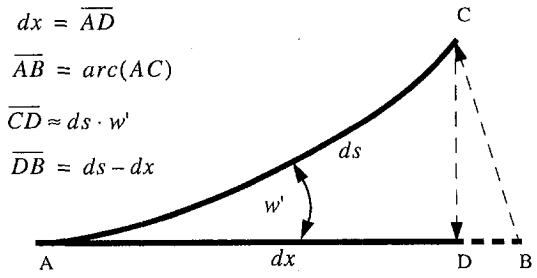

Fig. 7 Local deformation of the appendage

Table 1 Configuration parameters

Parameter	Symbol	Value
Hub radius	r	1.0 ft
Rotary inertia of hub	I_h	8.0 slug-ft^2
Mass density of beams	ρ	0.0271875 slug/ft
Elastic modulus of arm	E	0.1584×10^{10} lb/ft^2
Appendage length	L	4.0 ft
Appendage thickness	t	0.125 in.
Appendage height	h	6.0 in.
Mass of the tip	m_t	0.156941 slug
Rotatory inertia of the tip mass	I_t	0.0018 slug-ft^2
Momentum torquer	τ_{max}	2.0 ft-lb

The position vector R is now modified to include the foreshortening effect:

$$R = \left(r + \int_0^x (1 - \tfrac{1}{2}(w')^2)ds\right)\cdot \hat{i} + w\cdot \hat{j} \qquad (18)$$

The velocity of the typical deformed point under consideration is then

$$\dot{R} = \left(\left(r + \int_0^x (1 - \tfrac{1}{2}(w')^2)dx\right)\cdot\dot{\theta} + \dot{w}\right)\cdot\hat{j} - \left(w\cdot\dot{\theta} + \int_0^x w'\dot{w}'dx\right)\cdot\hat{i} \qquad (19)$$

where $\dot{\theta}$ is the angular velocity of the hub-fixed frame relative to the inertial frame.

Upon using the assumed mode method, the bending deflection $w(x, t)$ can be represented as

$$w(x, t) = \sum_{i=1}^{N} q_i(t)\phi_i(x) \qquad (20)$$

where $\phi_i(x)$ represents the ith assumed mode shape, $q_i(t)$ represents the ith generalized coordinate, and N represents the number of vibration modes. The admissible mode shape of this clamped-free appendage (clamped to the hub) that satisfies the geometrical boundary conditions (Junkins and Kim, 1993) is

$$\phi_i(x) = 1 - \cos\left(\frac{i\pi x}{L}\right) + \frac{1}{2}(-1)^{i+1}\left(\frac{i\pi x}{L}\right)^2 \qquad (21)$$

Only the first mode is considered in this analysis; therefore, N is assigned to 1.

The kinetic energy of the system is then given by

$$T = T_{hub} + T_{appendage} + T_{tip} \qquad (22)$$

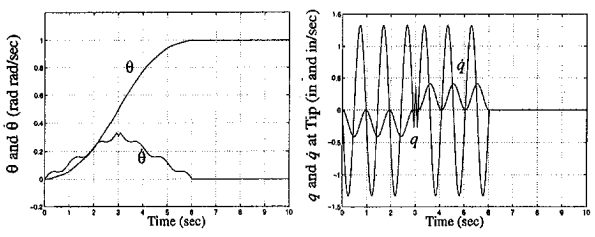

Fig. 8 Time-optimal control of flexible spacecraft maneuver with nominal stiffness

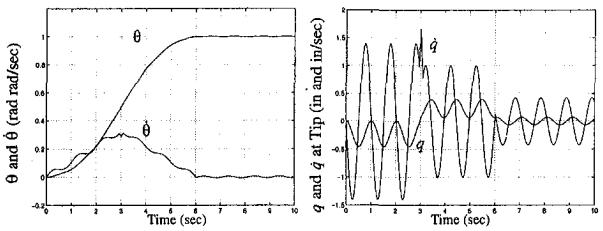

Fig. 9 Time-optimal control of flexible spacecraft maneuver with −10 percent stiffness

where

$$(1)\quad T_{hub} = \tfrac{1}{2}I_{hub}\dot{\theta}^2 \qquad (23)$$

$$(2)\quad T_{appendage} = \int_0^L \rho\left(\left(r + x - \tfrac{1}{2}q^2\int_0^x(\phi')^2dx\right)\dot{\theta} + \phi\dot{q}\right)^2 dx + \int_0^L \rho\left(\phi q\dot{\theta} + q\dot{q}\int_0^x(\phi')^2dx\right)^2 dx \qquad (24)$$

$$(3)\quad T_{tip} = m_t((r + L - \tfrac{1}{2}q^2(\phi'(L))^2)\dot{\theta} + \phi(L)\dot{q})^2 + m_t(\phi(L)q\dot{\theta} + (\phi'(L))^2q\dot{q})^2 + I_t(\dot{\theta} + \dot{w}'(L))^2 \qquad (25)$$

(4) I_{hub} is the moment of inertia of the rigid hub
(5) L is the length of the appendage
(6) ρ is the mass density per unit length of the appendage
(7) m_t is the mass of the tip, and
(8) I_t is the rotatory inertia of the tip mass.

The potential energy is

$$U = \int_0^L EI(w'')^2dx \qquad (26)$$

where E is the Young's modulus of the appendage, I is the area moment of inertia of the cross section about centroidal axis, and $w'' \equiv \partial^2 w/\partial x^2$.

The Euler-Lagrange equations of motion of the system can now be derived and are not listed here in the interest of brevity.

Table 1 summarizes the system parameters which are required to derive the equations of motion and are identical to those presented by Junkins and Kim (1993).

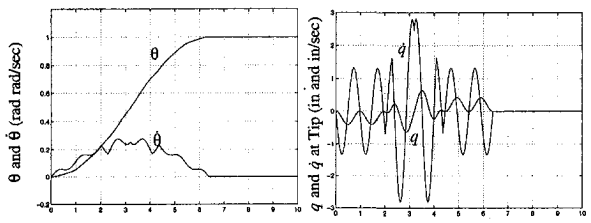

Fig. 10(*a*) Robust time-optimal control of flexible spacecraft maneuver with nominal stiffness

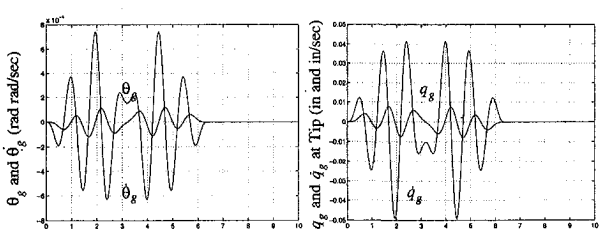

Fig. 10(*b*) Robust time-optimal control of flexible spacecraft maneuver with nominal stiffness

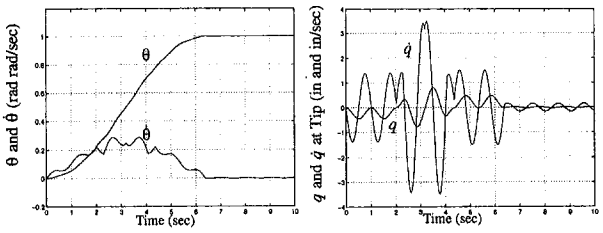

Fig. 11 Robust time-optimal control of flexible spacecraft maneuver with −10 percent stiffness

4.2 Robust Design. Let $\underline{x}$ denote $[\theta\ \dot{\theta}\ q\ \dot{q}]^T$ for the system described in Section 4.1. The sensitivity of the states $\underline{x}$ with respect to the system stiffness is

$$\underline{x}_g = \frac{d\underline{x}}{dk_{qq}}. \tag{27}$$

$$\dot{\underline{x}}_g = \frac{\partial \dot{\underline{x}}}{\partial k_{qq}} + \sum_{i=1}^{4} \frac{\partial \dot{\underline{x}}}{\partial x_i} \frac{\partial x_i}{\partial k_{qq}} \tag{28}$$

where $k_{qq} = \int_0^L EI(\phi'')^2 dx$ is the system stiffness.

The boundary conditions of the optimal control problem described in Section 2 are given as

$$\theta(0) = q(0) = \dot{\theta}(0) = \dot{q}(0) = 0,$$
$$\theta(t_f) = 1 \text{ rad}, \quad \text{and} \quad q(t_f) = \dot{\theta}(t_f) = \dot{q}(t_f) = 0 \tag{29}$$

for the nonrobust design and

$$\theta(0) = q(0) = \dot{\theta}(0) = \dot{q}(0) = 0,$$
$$\theta_g(0) = q_g(0) = \dot{\theta}_g(0) = \dot{q}_g(0) = 0,$$
$$\theta(t_f) = 1 \text{ rad/s}, \quad q(t_f) = \dot{\theta}(t_f) = \dot{q}(t_f) = 0, \quad \text{and}$$
$$\theta_g(t_f) = q_g(t_f) = \dot{\theta}_g(t_f) = \dot{q}_g(t_f) = 0 \tag{30}$$

for the robust case. Figures 8, and 9 present the evolution of the system states for the system subject to the nonrobust controller, for the cases with nominal value, and with minus 10 percent error of system stiffness, respectively. It is obvious from the plots (Fig. 9) of the deflection and velocity of the tip about the rigid body position, that there exists significant residual vibrations. Figures 10(a) and 10(b) illustrate the evolution of the system states, and the state sensitivities, respectively, for the robust time-optimal controller applied to the nominal system. It can be seen from Fig. 10(b) that all the state sensitivities are forced to zero at the final time. Figure 11 exemplifies the results for the robust design for minus 10 percent error in the system stiffness. It can be seen that there is significant improvement in reducing the residual vibrations compared to Fig. 9. The three switch nonrobust and the five switch robust control profiles are shown in Figs. 12 and 13. Comparisons of the maximum amplitude of hub and tip residual oscillation, with respect to variation of the normalized system frequency, are shown in Fig. 14. From these figures, it is seen that the residual oscillation have been reduced dramatically for the robust design compared with those of the nonrobust case, for both + or −10 percent deviation of system stiffness. Furthermore, the robust design is able to provide better result in the range of minus 13 to plus 25 percent deviation of the stiffness for this spacecraft, for rest-to-rest maneuvers.

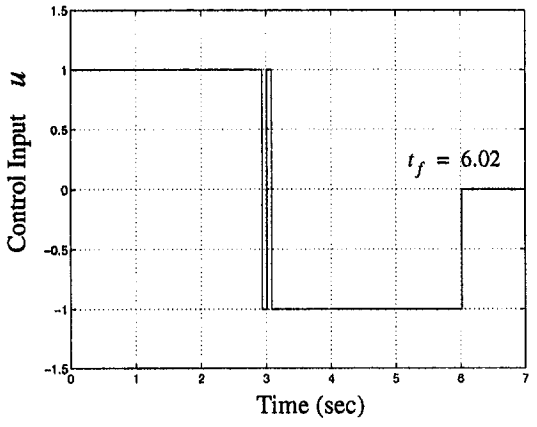

Fig. 12 Responses to time-optimal control input of flexible spacecraft maneuver

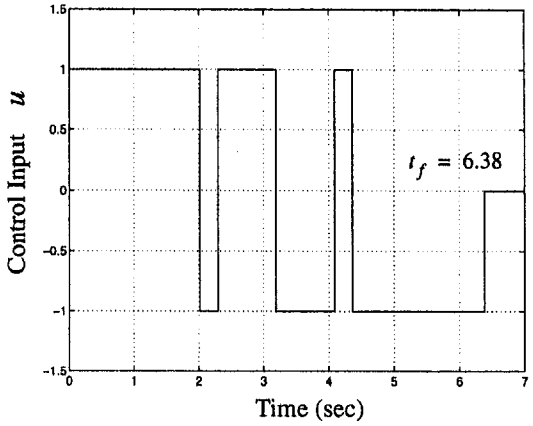

Fig. 13 Responses to robust time-optimal control input of flexible spacecraft maneuver

5 Conclusions

A new approach to design desensitized time-optimal controllers has been proposed which can be applied to both linear and nonlinear systems. The proposed approach is first applied to the benchmark spring-mass system and the resulting robust control profile is shown to be identical to that presented in the literature. The equation of motion of a slewing flexible structure is derived with the nonlinear effects due to foreshortening of the appendages included in the model in addition to the nonlinear effects due to rotation of two frame systems. Robust time-optimal controllers, which force the sensitivity of the system states with respect to the uncertain stiffness of the system to zero, are derived using the STO algorithm. Simulation results for both the linear and nonlinear

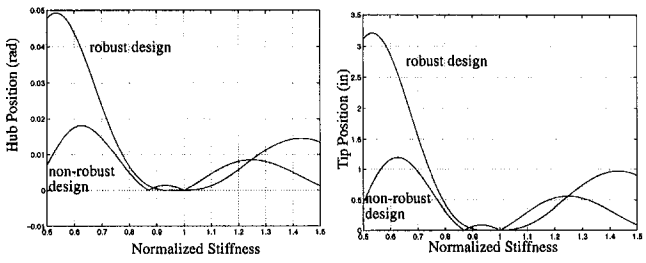

Fig. 14 Maximum amplitude of residual oscillation versus normalized stiffness

systems illustrate the significant reduction in the residual vibration of the structures.

References

Byers, R. M., Vadali, S. R., and Junkins, J. L., 1990, "Near-Minimum Time, Closed-Loop Slewing of Flexible Spacecraft," *Journal of Guidance, Control, and Dynamics,* Vol. 13, No. 1, Jan-Feb., pp. 57–65.

Junkins, J. L., and Kim, Y., 1993, *Introduction to Dynamics and Control of Flexible Structures,* AIAA Education Series, Published by AIAA, Inc., Washington, DC.

Liu, Q., and Wie, B., 1992, "Robust Time-Optimal Control of Uncertain Flexible Spacecraft," *Journal of Guidance, Control, and Dynamics,* Vol. 15, No. 3, May-June, pp. 597–604.

Meier, E-B., and Bryson, A. E., Jr., 1990, "Efficient Algorithm for Time-Optimal Control of a Two-Link Manipulator," *Journal of Guidance, Control, and Dynamics,* Vol. 13, No. 5, Sept.-Oct., pp. 859–866.

Scrivener, S., and Thompson, R. C., 1992, "Survey of Time-Optimal Attitude Maneuvers," American Astronomical Society/AIAA Spacecraft Mechanics Meeting, AAS Paper 92-168, Colorado Springs, CO., Feb. 24–26.

Singer, N. C., and Seering, W. P., 1990, "Preshaping Command Inputs to Reduce System Vibration," ASME JOURNAL OF DYNAMIC SYSTEMS, MEASUREMENT, AND CONTROL, Vol. 112, Mar., pp. 76–82.

Singh, G., Kabamba, P. T., and McClamroch, N. H., 1989, "Planar, Time-Optimal, Rest-to-Rest Slewing Maneuvers of Flexible Spacecraft," *Journal of Guidance, Control, and Dynamics,* Vol. 12, No. 1, Jan-Feb., pp. 71–81.

Singh, G., Kabamba, P. T., and McClamroch, N. H., 1990, "Time-Optimal Spinup Maneuvers of Flexible Spacecraft," *Journal of the Astronautical Sciences,* Vol. 38, No. 1, Jan-Mar., pp. 41–67.

Singh, T., and Vadali, S. R., 1994, "Robust Time-Optimal Control: Frequency Domain Approach," *Journal of Guidance, Control, and Dynamics,* Vol. 17, No. 2, Mar-Apr., pp. 346–353.

Singh, T., and Vadali, S. R., 1993, "Input Shaped Control of Three-Dimensional Maneuvers of Flexible Spacecraft," *Journal of Guidance, Control, and Dynamics,* Vol. 16, No. 6, pp. 1061–1068.